ACS APPLIED MATERIALS & INTERFACES

Research Article

www.acsami.org

Effect of Functional Groups on the Sensing Properties of Silicon Nanowires toward Volatile Compounds

Bin Wang and Hossam Haick*

The Department of Chemical Engineering and Russell Berrie Nanotechnology Institute, Technion-Israel Institute of Technology, Haifa 3200003, Israel

Supporting Information

ABSTRACT: Molecular layers attached to a silicon nanowire field effect transistor (SiNW FET) can serve as antennas for signal transduction of volatile organic compounds (VOCs). Nevertheless, the mutual relationship between the molecular layers and VOCs is still a puzzle. In the present paper, we explore the effect of the molecular layer's end (functional) groups on the sensing properties of VOCs. Toward this end, SiNW FETs were modified with tailor-made molecular layers that have the same backbone but differ in their end groups. Changes in the threshold voltage (ΔV_{th}) and changes in the mobility ($\Delta\mu_h$) were then recorded upon exposure to various VOCs. Model-based analysis indicates that the interaction between molecular layers and VOCs can be classified to three main scenarios: (a) dipole−dipole interaction between the molecular layer and the polar VOCs; (b) induced dipole−dipole interaction between the molecular layers and the nonpolar VOCs; and (c) molecular layer tilt as a result of VOCs diffusion. Based on these scenarios, it is likely that the electron-donating/withdrawing properties of the functional groups control the dipole moment orientation of the adsorbed VOCs and, as a result, determine the direction (or sign) of the ΔV_{th}. Additionally, it is likely the diffusion of VOCs into the molecular layer, determined by the type of functional groups, is the main reason for the $\Delta\mu_h$ responses. The reported findings are expected to provide an efficient way to design chemical sensors that are based on SiNW FETs to nonpolar VOCs, which do not exchange carriers with the molecular layers.

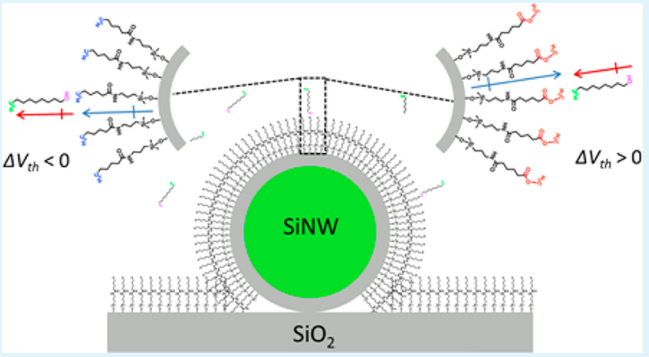

KEYWORDS: *silicon nanowire, field effect transistor, sensor, molecular layer, dipole*

INTRODUCTION

Silicon nanowires (SiNWs) offer unique opportunities for signal transduction that is linked with (semi)selective recognition of (bio)chemical species of interest.[1−5] The choice of SiNWs for sensing applications could be attributed to one or a combination of the following advantages: (i) the ease to grow (p-type and n-type) crystalline SiNWs; (ii) high surface-to-volume ratio and an efficient conductivity along the growth crystalline axis; (iii) almost all the as-grown SiNWs are semiconductors with (almost) uniform diameter, length, and shape; and (iv) SiNWs permit high carriers mobility and, as a result, high sensitivity to analytes adsorbed on their surfaces.[1−8] Nevertheless, for the majority of sensing applications under real-world conditions, the surfaces of SiNWs have to be molecularly engineered with (bio)chemical layers. This is because molecular modification of SiNWs is believed to deliberately control the stability, (surface) tarp states, and electrical properties of SiNWs and, also, the physical/chemical interaction between the SiNWs and analytes.[9−15]

Oxide-coated SiNW field effect transistors (FETs) were functionalized with amino silane molecular layers to impart relatively high sensitivity toward pH and with a variety of biological receptors to selectively detect biological species (e.g., DNA, proteins, viruses, etc.) in solution; see recent reviews[1−5] and references therein. Also, several studies have reported highly sensitive detection of polar gas analytes (e.g., N_2O, NO, CO, etc.) when SiNW FETs were used.[16−19] It has been accepted that the conductance of the molecularly modified SiNW FET sensors changes in response to variations in the electric field or the potential at the conduction channel's outer surface, which result from molecular gating, viz., the binding or adsorption of the (bio)molecules.[20−26] In contrast to the high sensing capabilities toward polar gas analytes, the detection of nonpolar gas analytes still remains difficult. For example, SiNW FETs coated with alkane-silanes, aldehyde-silanes, or amino-silanes gave different responses and sensitivity when exposed to hexane at 1000 ppm but have not shown sensing signals upon exposure to 40 ppb of the same analyte.[17] Recently, Paska et al. showed that controlling the cross-linking bonds between the adjacent alkyl silane molecules generates high signal-to-noise ratio upon exposing the molecularly modified SiNW FETs to nonpolar analytes.[21,22] It was proposed that the sensing of

Received: February 3, 2013
Accepted: March 2, 2013
Published: March 2, 2013

   dx.doi.org/10.1021/am4004649 | ACS Appl. Mater. Interfaces 2013, 5, 2289−2299

nonpolar analytes could be ascribed to molecular gating, due to two *indirect* effects. The first effect is attributed to changes in the charged surface states, mostly due to analyte-induced conformational changes in the organic monolayer that affect the density of charged surface states at the SiO_2/monolayer interface.[21,22] The second effect is attributed to changes in the dielectric medium (or condensed analytes) close to the SiNW surface.[21,22]

So far, the reported (response and sensitivity) improvements still far away from the performances required for successful detection of polar and nonpolar volatile organic compounds (VOCs) that exist in important real-world applications, such as detection of disease or oxidative stress products via breath and/or *in vitro* samples,[27−34] detection of explosive materials,[18] detection of environmental agents, etc. To improve the sensing performance toward important (fingerprints of) VOCs, one has to understand the effect/contribution of the molecular layers intrinsic properties, including but not confined to the effect/contribution of the molecular length, the backbone confirmation, the end (functional) group(s), and the anchor binding of the molecular layer with the SiNW surface.

Generally, the end groups of the molecular layers can serve as: (i) acceptor/donator antennas and/or as selective binding agents of biomolecules;[1−5] (ii) agents to deliberately control the electrical properties of the SiNW FETs;[25,35−41] and (iii) factors for determining the wettability of the SiNWs upon exposure to analytes.[9,42−44] However, the mutual relationship between the end groups of molecular layers and the VOCs, especially the nonpolar ones, is still a puzzle. In the present paper, we will focus on understanding the effect of the end (functional) group of the molecular layer on the sensing properties of the SiNW FETs.Toward achieving the stated goals, SiNW FETs were modified with tailor-made molecular layers that have the same backbone but differ in their end groups (see Figure 1). Changes in the threshold voltage (ΔV_{th}) and changes in the mobility ($\Delta\mu_h$) were then recorded upon exposure to various polar and nonpolar VOCs under various conditions. Our results show that the molecularly modified SiNW FETs exhibit excellent ΔV_{th} and $\Delta\mu_h$ responses and reversibility upon exposure to both polar and nonpolar VOCs. In addition, ΔV_{th} and $\Delta\mu_h$ show clear dependence on the concentration of VOCs, and the shift direction of V_{th} is dependent on the end groups of the molecular layers. On the basis of the experimental results, a model that is based on dipole sensing is proposed as a way to explain the sensing mechanism.

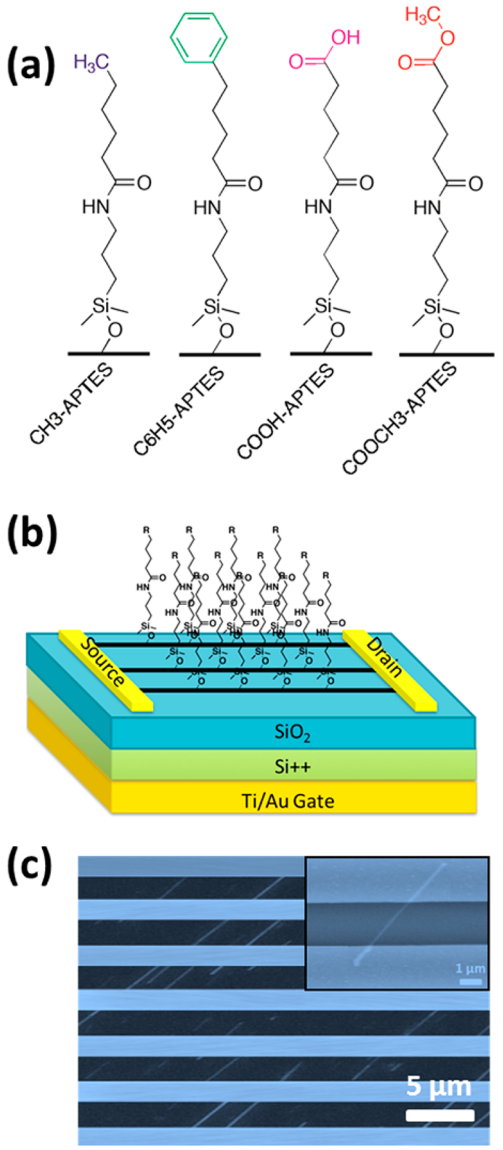

Figure 1. (a) Schematic illustration of molecular layer with different functional groups on the SiNW surface. (b) Schematic illustration of molecularly modified SiNW FET sensor. (c) Typical scanning electron microscopy image of SiNWs array contacted within the FET platform.

EXPERIMENTAL SECTION

Synthesis of SiNWs. P-type SiNWs with an average diameter of 40 ± 8 nm and an average length of 8.5 ± 1.5 μm were grown on Si wafers by chemical vapor deposition using SiH_4 and B_2H_6 (1:20000 of B/Si ratio) as precursor gases and gold as catalyst.[45] The as-grown SiNWs consisted almost entirely of single-crystalline Si core coated with 5 ± 1 nm of native SiO_x layer. More details on the SiNWs synthesis and properties could be found elsewhere.[45]

Deposition of SiNW Arrays. The as-grown SiNWs were first etched in buffered hydrofluoric acid for 15 s and in $KI/I_2/H_2O$ (mass ratio 4:1:40) solution for 2 min, to remove (i) the gold catalyst used during the growth process, (ii) the native SiO_x, and (iii) possible gold contaminants on the SiNW surface. Following the initial pretreatment process, the SiNWs were dispersed in ethanol, using ultrasonication for 6 s. The dispersed SiNWs exhibited, probably due to the ultrasonic process, relatively higher length distribution (4−10 μm) than the SiNWs attached to growth batch (7−10 μm). SiNWs dispersed in ethanol were deposited on a precleaned p-Si(100) (0.001Ω·cm resistivity) "receiver" substrate with 300 nm thermal oxide and a Ti/Au (10/200 nm) bottom gate electrode. The deposition method used in the current study was based on a spray-coating process under controlled conditions that was reported elsewhere.[46,47] Briefly, the deposition of the SiNWs started with the placement of the "receiver" substrate on a hot plate at 75 °C. The suspension of SiNWs was then applied using a spray gun (Prona R2-F) with 40 psi carrier gas (nitrogen) pressure and with a tilting angle of 5° ± 2° relative to the "receiver" substrate. The nozzle tip was usually held at a distance of 1 cm from the substrate. This process generated a well-aligned array of NWs with density of ∼1 NW/100 μm^2.

Fabrication of SiNW FETs. Prior to the device fabrication, the top substrate was cleaned by ultrasonic treatment in acetone, methanol, and ethanol and slightly etched using oxygen plasma (50 W; 1 min) for removing residues of organic contaminations. Eighteen pairs of 1300 μm long and 2 μm wide interdigitated Ti/Au (40/110 nm) source/drain (S/D) electrodes with an interelectrode spacing of 2 μm were defined on top of the sprayed SiNW array using photolithography (Karl Suss MA6Mask Aligner). The native oxide on the

SiNWs that are designated to exist beneath the metallic contact was etched by buffered hydrofluoric acid for 5 s immediately before being loaded into the metal deposition system. The metal contacts were applied by a conventional lift-off process. The number of bridged SiNWs between the S/D electrodes was evaluated by an optical microscope (Olympus BX51RF-5) in dark field mode or scanning electron microscope (e-LiNE, Raith, Dortmund, Germany).[46,47]

Molecular Modification of SiNW FETs. 3-Aminopropyl-triethoxylsilane (APTES), hexanoyl chloride (HEC), 1,4-butanedicarbonyl chloride (BUC), and methyl adipoly chloride (MEAC) were bought from Sigma-Aldrich. 5-Phenylvaleric chloride (PHC) was synthesized as described in the Supporting Information. The surface of SiNW FETs were activated using a 60 s oxygen plasma treatment. These devices were immersed in a solution of APTES in dehydrated ethanol (10 mM, 20 mL) at room temperature for 60 min. Then, the APTES-terminated SiNW FETs (herewith, APTES-SiNW FET) were rinsed thoroughly with acetone, ethanol, and isopropanol and dried by N_2 flow. APTES-SiNW FETs were immersed in a solution of acyl chloride (10 mM) in chloroform with 10 μL of triethylamine for 17 h. APTES-SiNW FETs modified with BUC were put into 90 °C hot water for 2 h to hydrolyze the end acyl chloride groups. These molecular layers have a common backbone but differ with their exposed end (functional) groups. Self-assembled monolayers of APTES that were further functionalized with $-CH_3$, $-C_6H_5$, $-COOH$, and $-COOCH_3$ end groups were named as CH_3-APTES, C_6H_5-APTES, COOH-APTES, and $COOCH_3$-APTES, respectively; see Figure 1a. To assess the electrical characteristics of SiNW FET devices before and after surface modification, S/D current (I_{ds}) versus back-gate voltage (V_g) measurements, swept backward between +40 and −40 V with 200 mV steps and at 2 V S/D voltage (V_{ds}), were carried out under ambient conditions using an Agilent B1500A Semiconductor device analyzer.

Characterization of the Molecularly Modified SiNW Surfaces. For X-ray photoelectron spectroscopy (XPS) and Kelvin Probe measurements, dense SiNW mats were deposited on Al film surface (200 nm thick e-beam evaporated Al film on planar Si wafer surface) by spray coating (Figure S1, Supporting Information). Then, spray coated SiNW mats were functionalized with APTES and a variety of functional groups, using the same method applied for the molecularly modified SiNW FETs. Surface analysis of the molecularly modified SiNW surfaces was carried out as described elsewhere.[20−22] Briefly, the molecularly modified SiNWs were characterized by high-resolution XPS (Thermo VG Scientific, Sigma probe, England) fitted with a monochromatized X-ray Al Kα (1486.6 eV) source.[20,21] Spectra analysis was performed using the peak fitting software (XPSPEAK version 4.1) after a shirly background subtraction. The C 1s (C−C) peak at 285.0 eV was used as reference for binding energy calibration. Work functions (Φ) of bare SiNWs and molecularly modified SiNW samples were measured using a Farady caged Kelvin Probe Package (KP Technology Ltd., UK) under N_2 atmosphere.[20,21] The work function resolution of the KP system is 1−3 mV. To make an Ohmic connection with an Al sample stage, samples were contacted on the back by applying InGa eutectic after scratching their surface with a diamond knife. The work function values were calibrated by high ordered pyrolytic graphite (HOPG; work function = 4.6 eV). Each surface analysis was repeated three times, and the averaged results were taken for further consideration. Since spectroscopic ellispsometry characterization of SiNWs is still technically challenging, surface analysis of molecular layers was carried out on top of the molecular layer modified planar Si(111) substrates. Briefly, planar Si(111) substrates with 1.7 ± 0.3 nm native oxide were functionalized with APTES and a variety of functional groups, using the same method applied for the molecularly modified SiNW FETs. The thickness of each molecular layer was determined by spectroscopic ellipsometer (M-2000 V, J. A. Woollam Co., Inc.) at five incidence angles (60°, 65°, 70°, 75°, and 80°) on an open sample stage.[20,21] Three-phase monolayer/native SiO_2/Si substrate model was used to extract the thickness of molecular layers. An absorption-free Cauchy dispersion of the refractive index with values of n between 1.46 at 1000 nm and 1.61 at 250 nm was assumed for all molecular modification layers. For the sake of comparison, the theoretical lengths of the various molecular layers were estimated with the help of Chem3D software.

Sensing Measurements of the Molecularly Modified SiNW FETs. Molecularly modified SiNW FETs with various functional groups, APTES-SiNW FET, and bare SiNW FET (without surface modification) were integrated into TO5 holders by wire-binding. The bonded devices were then mounted on a custom circuit board with 20 separated sensor sites and put in a stainless steel test chamber with ~170 cm^3 volume. Sensing measurements of VOCs were performed using a Keithley 2636A system SourceMeter and Keithley 3706 system Switch/Multimeter. I_{ds} versus V_g measurements, swept backward between +40 and −40 V with 200 mV steps and at 2 V V_{ds}, were carried out, before, during, and after exposure to VOCs. Table 1 lists

Table 1. Physical Properties of the Volatile Organic Compounds (VOCs) Used for the Exposure Experiments[51]

VOC	formula	p_o (kPa)[a]	ε^v	dipole moment (Debye)	density ($g \cdot cm^{-3}$)
n-hexane	$CH_3(CH_2)_4CH_3$	17.60	1.89	0	0.655
n-octane	$CH_3(CH_2)_6CH_3$	1.47	1.94	0	0.703
n-decane	$CH_3(CH_2)_8CH_3$	1.58	1.98	0	0.730
ethanol	CH_3CH_2OH	5.95	24.3	1.69	0.789
1-hexanol	$CH_3(CH_2)_5OH$	0.95	13.03	1.65	0.814
1-octanol	$CH_3(CH_2)_7OH$	0.11	10.3	1.76	0.824
1-decanol	$CH_3(CH_2)_9OH$	0.015	7.93	1.68	0.830

[a]Values at 20 °C.

the polar and nonpolar VOCs that were examined in the current study (see Table 1). Vapors of targeted VOCs were produced by bubbling air through their liquid states, using glass bubblers and diluted with a flow of carrier air. Oil-free, purified dry air (8−10% relative humidity) was used as a reference gas as well as a carrier gas for the VOCs. The background humidity was introduced as a real-world confounding factor.[48−50] The sensing responses to single VOC were tested by introducing the VOC vapors to test chamber with a 5 L/min constant flow. Signals were collected for 30 min under air flow, preceded by 30 min under flowing VOC vapor. The cycles were repeated four times at four successively increasing concentrations, from p_a/p_o = 0.01 to 0.08 (where p_a and p_o stand for the VOC's partial pressure and vapor pressure at a given temperature, respectively).

RESULTS

Characterization of Modified Molecular Layers. Spectroscopic ellipsometry was used for evaluating the thickness of the molecular layers on the SiNW surfaces. Since spectroscopic ellipsometry is still technically challenging in nanoscale objects, it was carried out on top of bare and molecular layers attached to the (native) SiO_2/Si (111) planar substrates. Table 2 summarizes the obtained thickness data of the molecularly modified (native) SiO_2/Si (111) samples. The measured thicknesses of the molecular layers were found to correspond with their calculated values, implying that they are at the monolayer level. The small standard deviations of the measured thicknesses suggest that the molecular layers were almost homogeneous.

XPS analysis was carried out for all samples. Since all molecular layers have the same APTES layer (see Experimental Section), we focus the analysis on the bridged amide bond characters. Figure S2 of the Supporting Information shows the XPS N1s spectra of the APTES-SiNW surface as well as the various molecularly modified APTES-SiNW samples. N1s of the APTES could be deviated into two peaks. The peak at 399.6

Table 2. Experimental and Theoretical Thickness of the Tested Molecular Modifications with Different Functional Groups

	functional group				
thickness of the molecular layer	APTES	CH_3-APTES	C_6H_5-APTES	COOH-APTES	$COOCH_3$-APTES
measured, Å	6.7 ± 0.3	12.9 ± 0.2	16.7 ± 0.1	12.3 ± 0.4	14.6 ± 0.4
calculated, Å	6.2	13.8	16.0	14.7	15.3

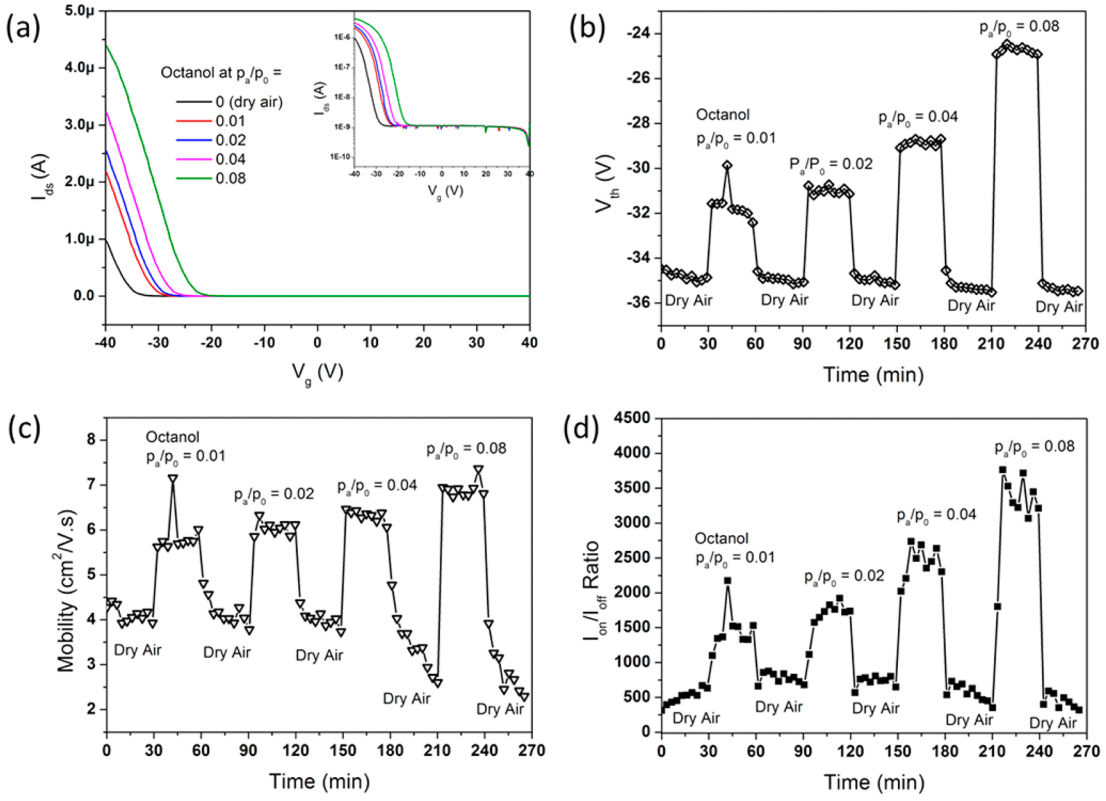

Figure 2. (a) Linear and logarithmic scale (inset) $I_{ds}-V_g$ curves of a $COOCH_3$-SiNW FET at different octanol concentrations. Time dependent response of $COOCH_3$-SiNW FET, as expressed by: (b) V_{th}; (c) average hole mobility per nanowire; and (d) I_{on}/I_{off} ratio upon exposure to octanol at different concentrations.

eV (54.0% peak area ratio) was attributed to neutral nitrogen, and the peak at 401.8 eV (46.0% peak area ratio) was attributed to positively charged nitrogen ($-NH_3^+$).[52] The positively charged nitrogen could be attributed to hydrogens that were transferred from surface hydroxyl (−OH) groups to part of APTES amino ($-NH_2$) groups. After reacting with acyl chlorides, the N 1s peak at 399.6 eV shifted to ~0.4 eV to the higher binding energy side. Since the peak of $-NH_3^+$ was linked to $-NH_2$, the positively charged nitrogen N1s peak could be used to monitor the reaction ratio of the second layer. For CH_3-APTES and $COOCH_3$-APTES, the N1s peak of $-NH_3^+$ disappeared, implying that nearly all $-NH_2$ reacted with acyl chlorides and formed amide bonds. However, for C_6H_5-APTES and COOH-APTES, the N1s peak of $-NH_3^+$ counted about 16.6% and 48.3% area ratio of the total N1s signals, respectively. For C_6H_5-APTES, the low reaction ratio of the second layer could be attributed to the steric effect of end phenol groups. For COOH-APTES, the low reaction ratio of the second layer could be attributed to the decomposition of some amide bonds in the hydrolyzing step.

Electrical and Sensing Characterization of SiNW FETs. Figure 2a shows the representative I_{ds} versus V_g characteristics of a SiNW FET modified with $COOCH_3$-APTES (herewith, $COOCH_3$-SiNW FET) upon exposure to various concentrations of octanol. For the sake of clear presentation, only one $I_{ds}-V_g$ curve was selected in each exposure step. As shown in the figure, $I_{ds}-V_g$ curves shifted to the right when exposed to octanol. The higher the octanol concentration, the larger were the $I_{ds}-V_g$ shifts. In addition, the on-current (I_{on}), which is defined as I_{ds} value at V_g = −40 V in the current paper, increased from 2.17 to 4.39 μA upon increasing the octanol concentration from p_a/p_o = 0.01 to 0.08. To further investigate the sensing responses, voltage threshold (V_{th}) and hole mobility (μ_h) were extracted from the extrapolation of the linear part of the $I_{ds}-V_g$ curves. Meanwhile, the on-current/off-current (I_{on}/I_{off}) ratio, which is defined as the ratio of I_{ds} at V_g= −40 and +40 V, was also calculated. Then, V_{th}, μ_h, and I_{on}/I_{off} ratio were plotted as function of time. As shown in Figure 2b−d, exposure of $COOCH_3$-SiNW FET to octanol shifted the V_{th} to higher positive values. The higher the octanol concentration, the higher was the V_{th} upon exposure to octanol, as compared to the dry air (baseline). We found that the V_{th} of $COOCH_3$-SiNW FET response was rapid, fully reversible, and responsive to a wide variety of concentrations. The μ_h and I_{on}/I_{off} ratio of the $COOCH_3$-SiNW FET showed similar behavior to the V_{th}.

Changes in Threshold Voltage of SiNW FETs upon Exposure to VOCs. Change in the V_{th} (herewith, ΔV_{th}) is calculated according to the following relationship:

dx.doi.org/10.1021/am4004649 | ACS Appl. Mater. Interfaces 2013, 5, 2289−2299

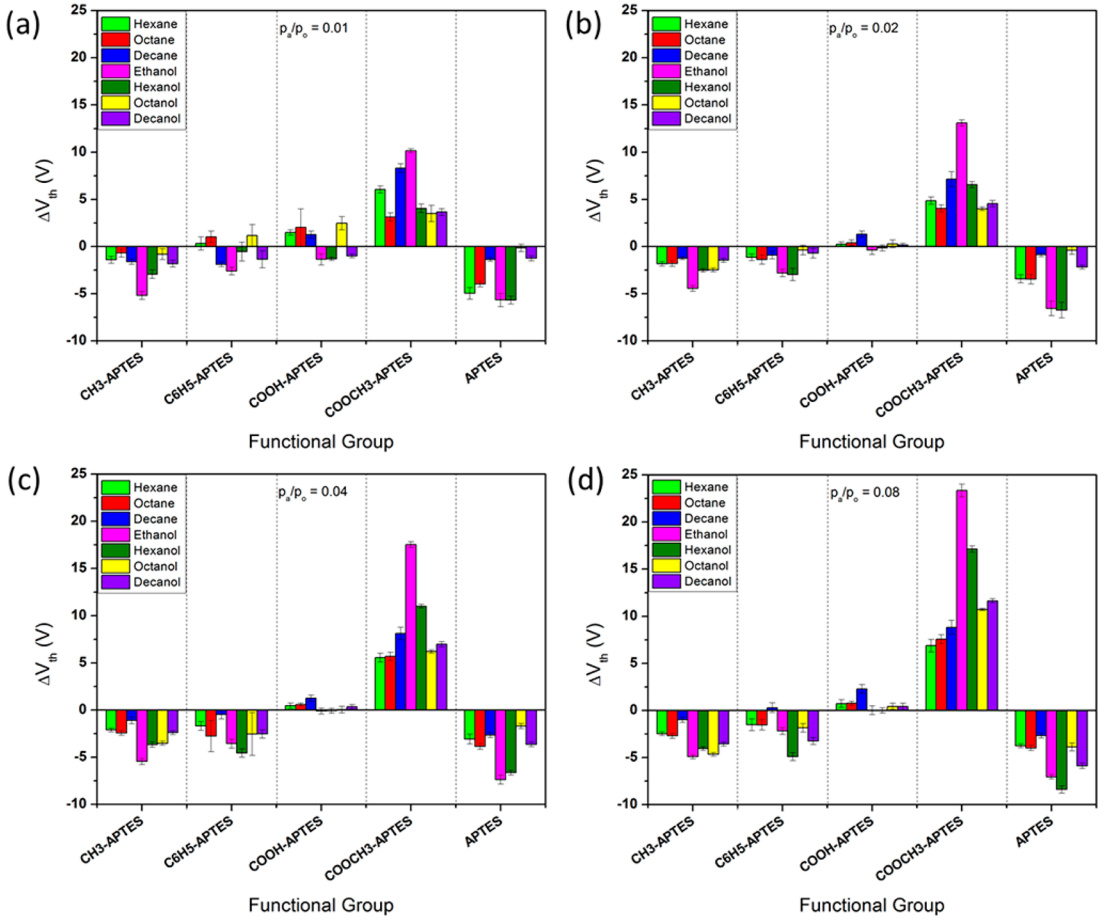

Figure 3. ΔV_{th} of APTES-SiNW FETs, with and without modifications with various functional groups, upon exposure to nonpolar alkyls and polar alcohols at: (a) p_a/p_o = 0.01; (b) p_a/p_o = 0.02; (c) p_a/p_o = 0.04; and (d) p_a/p_o = 0.08. ΔV_{th} of the bare SiNW FET (without surface modification) is presented in the Supporting Information, Figure S3a.

$$\Delta V_{th} = V_{th\text{-}e} - V_{th\text{-}a} \quad (1)$$

where $V_{th\text{-}e}$ is the mean value of V_{th} during exposure to VOC and $V_{th\text{-}a}$ is the mean value of V_{th} in a reference air. At the beginning, the ΔV_{th} of two reference devices, viz., bare SiNW FET and APTES-SiNW FET, were calculated and analyzed. As seen in Figure S3a of the Supporting Information, the bare SiNW FET showed no clear ΔV_{th} response to VOCs and/or concentrations. Attaching APTES chemical antennas to the bare SiNW FET (herewith, APTES-SiNW FET) improved the ΔV_{th} response to VOCs and/or concentrations. As seen in Figure 3, APTES-SiNW FET showed negative ΔV_{th} to all polar and nonpolar VOCs, at all tested concentrations. For nonpolar VOCs at p_a/p_o = 0.01, exposure of APTES-SiNW FET to hexane led to the largest ΔV_{th} (−4.96 ± 0.62 V), while exposure to decane led to the smallest ΔV_{th} (−1.38 ± 0.19 V). For polar VOCs at p_a/p_o = 0.01, exposure of APTES-SiNW FET to hexanol led to the largest ΔV_{th} (−5.68 ± 0.42 V), while exposure to decanol led to the smallest ΔV_{th} (−1.25 ± 0.27 V). APTES-SiNW FET showed no response to octanol at $p_a/p_o \leq$ 0.02. At p_a/p_o = 0.04, APTES-SiNW FET showed negative ΔV_{th} (−1.70 ± 0.28 V) to octanol. Excluding decanol, the ΔV_{th} of APTES-SiNW FET showed no clear dependence with the VOC concentration.

SiNW FET modified with CH_3-APTES (herewith, CH_3-SiNW FET) showed negative ΔV_{th} to all polar and nonpolar VOCs at all tested concentrations. At p_a/p_o = 0.01, exposure of CH_3-SiNW FET to decane led to the largest ΔV_{th} (−1.62 ± 0.28 V), while exposure to octane led to the smallest ΔV_{th} (−0.69 ± 0.43 V). Increasing the hexane concentration from p_a/p_o = 0.01 to 0.08 increased the ΔV_{th} of CH_3-SiNW FET from −1.41 ± 0.36 to −2.47 ± 0.20 V. Increasing the octane concentration from p_a/p_o = 0.01 to 0.08 increased the ΔV_{th} of CH_3-SiNW FET from −0.69 ± 0.43 to −2.70 ± 0.27 V. In contrast, increasing the decane concentration from p_a/p_o = 0.01 to 0.08 decreased the ΔV_{th} of CH_3-SiNW FET from −1.62 ± 0.43 to −0.99 ± 0.28 V. Altogether, the ΔV_{th} of CH_3-SiNW FET obeyed the following sequence: $(\Delta V_{th})_{octane} > (\Delta V_{th})_{hexane} > (\Delta V_{th})_{decane}$. For polar VOCs, exposure of the CH_3-SiNW FET to ethanol led to the largest ΔV_{th} (−5.19 ± 0.41 V), while exposure to octanol led to the smallest ΔV_{th} (−0.82 ± 0.56 V) at p_a/p_o = 0.01. Increasing the p_a/p_o from 0.01 to 0.08 increased the ΔV_{th} of CH_3-SiNW FET to hexanol, octanol, and decanol (−4.05 ± 0.22, −4.66 ± 0.19, and −3.56 ± 0.23 V, respectively). In contrast, the ΔV_{th} of CH_3-SiNW FET to ethanol decreased by 0.3 V from p_a/p_o = 0.01 to 0.08. Nevertheless, considering the relatively large standard deviation of the ΔV_{th}, these small ΔV_{th} can be neglected. Comparing polar and nonpolar VOCs with similar chain length at a specific concentration showed that polar VOCs always generated higher ΔV_{th}. The higher the VOC concentration, the higher were the absolute values of ΔV_{th} (i.e., $|\Delta V_{th}|$). For polar VOCs, the higher the chain length, the lower was the $|\Delta V_{th}|$.

dx.doi.org/10.1021/am4004649 | ACS Appl. Mater. Interfaces 2013, 5, 2289−2299

SiNW FET modified with C_6H_5-APTES (herewith, C_6H_5-SiNW FET) showed negative ΔV_{th} upon exposure to decane (-1.89 ± 0.25 V) and ethanol (-2.60 ± 0.41 V) at p_a/p_o = 0.01. However, it showed no ΔV_{th} to other VOCs at p_a/p_o = 0.01, because its standard deviation was larger than its mean value. For part of the VOCs, increasing the p_a/p_o led to weak negative ΔV_{th}. Excluding decane, the higher the VOC concentration, the higher was the negative ΔV_{th} of the C_6H_5-SiNW FET. Due to the weak ΔV_{th} responses of C_6H_5-SiNW FET, no conclusions can be drawn in VOC chain length dependent response.

SiNW FET modified with COOH-APTES (herewith, COOH-SiNW FET) showed positive ΔV_{th} upon exposure to hexane (1.50 ± 0.28 V), decane (1.26 ± 0.37 V), and octanol (2.47 ± 0.69 V). In contrast, the same device showed negative ΔV_{th} upon exposure to ethanol (-1.37 ± 0.50 V), hexanol (-1.31 ± 0.18 V), and decanol (-1.01 ± 0.20 V) at p_a/p_o = 0.01. Exposure of COOH-SiNW FET to nonpolar VOCs showed no clear dependence between the ΔV_{th} and VOC concentration. At p_a/p_o = 0.08, exposure of COOH-SiNW FET to decane exhibited the largest response (2.29 ± 0.47 V) and near equal response to hexane (0.73 ± 0.40 V) and octane (0.76 ± 0.23 V). In contrast, COOH-SiNW FET could detect only polar VOCs in p_a/p_o = 0.01. For $p_a/p_o \geq 0.02$, the COOH-SiNW FET showed negligible ΔV_{th} as well as drift in the baseline (see Supporting Information, Figure S4).

SiNW FET modified with $COOCH_3$-APTES (herewith, $COOCH_3$-SiNW FET) showed strong positive ΔV_{th} for all polar and nonpolar VOCs at all examined concentrations. At p_a/p_o = 0.01, exposure of $COOCH_3$-SiNW FET to decane exhibited the largest ΔV_{th} (8.30 ± 0.47 V). In contrast, exposure of $COOCH_3$-SiNW FET to octane exhibited the smallest ΔV_{th} (3.12 ± 0.44 V). For polar VOCs, the ΔV_{th} ranged between 3.66 ± 0.36 V in the case of decanol to 10.15 ± 0.20 V in the case of ethanol. The higher the VOC concentration, the higher was the ΔV_{th}. At $p_a/p_o \geq 0.04$, the higher the chain length of the nonpolar VOCs, the higher was the ΔV_{th}. In contrast, at $p_a/p_o \geq 0.04$, the higher the chain length of the polar VOCs, the lower was the ΔV_{th}. For a specific chain length and VOC concentration, exposure of the $COOCH_3$-SiNW FET to polar VOCs exhibited higher ΔV_{th} than nonpolar VOCs.

To summarize this section, SiNW FETs modified with different functional groups showed different ΔV_{th} sensitivity toward exposure to VOCs. Upon exposure to a specific VOC, $COOCH_3$-SiNW FET showed the strongest ΔV_{th}, followed, in succession, by CH_3-SiNW FET, C_6H_5-SiNW FET, and COOH-SiNW FET.

Changes in Hole Mobility of SiNW FETs upon Exposure to VOCs. Change in hole mobility ($\Delta\mu_h$) is given by:

$$\Delta\mu_h = \mu_{h\text{-}e} - \mu_{h\text{-}a} \quad (2)$$

where $\mu_{h\text{-}e}$ is the mean value of μ_h at a given VOC exposure step and $\mu_{h\text{-}a}$ is the mean value of μ_h in a reference air. At the beginning, the $\Delta\mu_h$ of two reference devices, viz., bare SiNW FET and APTES-SiNW FET, were calculated and analyzed. As seen in Figure S3b in the Supporting Information, the bare SiNW FET showed weak positive $\Delta\mu_h$ response to ethanol (0.13 ± 0.03 $cm^2/V{\cdot}s$ to 0.16 ± 0.04 $cm^2/V{\cdot}s$) at $0.01 \leq p_a/p_o \leq 0.08$. For the rest of VOCs, the bare SiNW FET showed only weak to negligible $\Delta\mu_h$ responses. Additionally, the bare SiNW FET showed no clear trend with VOC concentration. Attaching APTES molecular layer to the bare SiNW FET (herewith, APTES-SiNW FET) improved the $\Delta\mu_h$ response to VOCs and/or concentrations (Figure 4). For nonpolar VOCs at p_a/p_o = 0.01, APTES-SiNW FET exhibited the largest $\Delta\mu_h$ to octane (0.59 ± 0.06 $cm^2/V{\cdot}s$) and the smallest $\Delta\mu_h$ to decane (0.12 ± 0.04 $cm^2/V{\cdot}s$). No clear trend between the $\Delta\mu_h$ and nonpolar VOC concentrations could be identified. For polar VOCs at p_a/p_o = 0.01, exposure of APTES-SiNW FET to ethanol led to the largest $\Delta\mu_h$ (0.97 ± 0.08 $cm^2/V{\cdot}s$), while exposure to decanol led to the smallest $\Delta\mu_h$ (0.14 ± 0.06 $cm^2/V{\cdot}s$). Increasing the concentration from p_a/p_o = 0.01 to 0.08, increased the $\Delta\mu_h$ upon exposure to ethanol, hexanol, and decanol by 0.44, 0.68, and 0.68 $cm^2/V{\cdot}s$, respectively. APTES-SiNW FET showed no response to octanol at $p_a/p_o \leq 0.02$ but did show a weak response at p_a/p_o = 0.04 ($\Delta\mu_h = 0.18 \pm 0.06$ $cm^2/V{\cdot}s$) and above.

Upon exposure to nonpolar VOCs at p_a/p_o=0.01, CH_3-SiNW FET showed the largest $\Delta\mu_h$ (0.99 ± 0.10 $cm^2/V{\cdot}s$) upon exposure to decane and the smallest $\Delta\mu_h$ (0.43 ± 0.10 $cm^2/V{\cdot}s$) upon exposure to octane. Increasing the concentration of octane and decane from p_a/p_o = 0.01 to p_a/p_o = 0.08 increased the $\Delta\mu_h$ by 0.63 and 0.49 $cm^2/V{\cdot}s$, respectively. On the other hand, increasing the concentration of hexane from p_a/p_o = 0.01 to p_a/p_o = 0.08 led to $\Delta\mu_h$ of 0.04 $cm^2/V{\cdot}s$, a value that was significantly smaller than the standard deviation of measured data (± 0.08 $cm^2/V{\cdot}s$). Upon exposure to nonpolar VOCs at $p_a/p_o \geq 0.04$, the higher the VOC's chain length, the higher was the $\Delta\mu_h$ of CH_3-SiNW FET. For polar VOCs, the $\Delta\mu_h$ of CH_3-SiNW FET ranged between 0.50 ± 0.05 $cm^2/V{\cdot}s$ upon exposure to octanol and 1.97 ± 0.13 $cm^2/V{\cdot}s$ upon exposure to ethanol. Additionally, the $\Delta\mu_h$ of CH_3-SiNW FET for polar VOCs showed strong dependence on the concentration. Increasing the concentration of ethanol, hexanol, octanol, and decanol from p_a/p_o = 0.01 to p_a/p_o = 0.08 increased the $\Delta\mu_h$, respectively, by 1.71, 1.55, 0.86, and 0.90 $cm^2/V{\cdot}s$. For polar VOCs, the higher the chain length, the lower was the obtained $\Delta\mu_h$.

Exposure of C_6H_5-SiNW FET to nonpolar VOCs at p_a/p_o = 0.01 showed weak $\Delta\mu_h$ to decane (0.34 ± 0.06 $cm^2/V{\cdot}s$) and no response to hexane and octane. Increasing the concentration of these two VOCs resulted in weak $\Delta\mu_h$. For polar VOCs, C_6H_5-SiNW FET showed weak $\Delta\mu_h$ (0.29 ± 0.07 $cm^2/V{\cdot}s$) upon exposure to ethanol but negligible $\Delta\mu_h$ upon exposure to other polar VOCs. At p_a/p_o = 0.02, a small $\Delta\mu_h$ (0.18 ± 0.03 $cm^2/V{\cdot}s$) was observed for hexanol. Weak responses for octanol (0.16 ± 0.03 $cm^2/V{\cdot}s$) and decanol (0.22 ± 0.03 $cm^2/V{\cdot}s$) were observed until p_a/p_o = 0.08.

Exposure of COOH-SiNW FET to nonpolar VOCs at p_a/p_o = 0.01 showed weak $\Delta\mu_h$ response to hexane (0.15 ± 0.06 $cm^2/V{\cdot}s$) and no $\Delta\mu_h$ response to octane and decane. At p_a/p_o = 0.04, a small $\Delta\mu_h$ (0.12 ± 0.03 $cm^2/V{\cdot}s$) was observed for octane. However, COOH-SiNW FET showed no $\Delta\mu_h$ response to decane at all examined concentrations. For polar VOCs, exposure of the COOH-SiNW FET to ethanol led to the largest $\Delta\mu_h$ (0.47 ± 0.05 $cm^2/V{\cdot}s$) at p_a/p_o= 0.01. The $\Delta\mu_h$ responses to polar VOCs increased with VOC concentration and showed decreasing trend with the increase of the VOC chain length.

Exposure of $COOCH_3$-SiNW FET to hexane and decane at p_a/p_o = 0.01 showed $\Delta\mu_h$ of 0.66 ± 0.20 and 0.59 ± 0.22 $cm^2/V{\cdot}s$, respectively. The $\Delta\mu_h$ of $COOCH_3$-SiNW FET showed no clear trend with hexane and octane concentrations. On the other hand, the $COOCH_3$-SiNW FET showed no response to decane at all examined concentrations. The response of

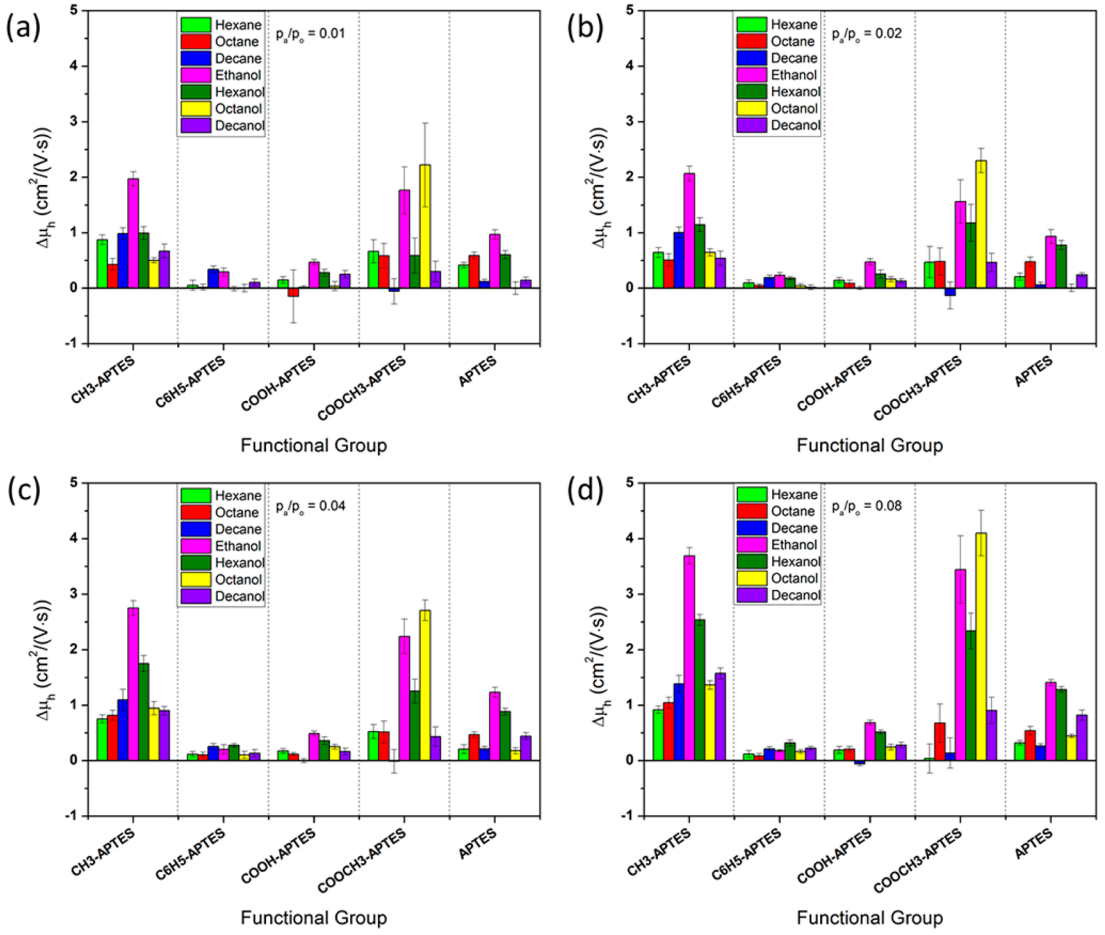

Figure 4. Change in hole mobility ($\Delta\mu_h$) of bare and molecularly modified SiNW FETs upon exposure to nonpolar alkyls and polar alcohols at: (a) p_a/p_o = 0.01; (b) p_a/p_o = 0.02; (c) p_a/p_o = 0.04; and (d) p_a/p_o = 0.08. $\Delta\mu_h$ of the bare SiNW FET (without surface modification) is presented in the Supporting Information, Figure S3b.

$COOCH_3$-SiNW FET showed strong dependence on the concentration of polar VOCs; i.e., $\Delta\mu_h$ increased with the increasing VOC concentration. Excluding octanol, which exhibited the largest $\Delta\mu_h$ among polar VOCs, the longer the VOC chain length, the lower was the $\Delta\mu_h$ upon exposure of the $COOCH_3$-SiNW FET to polar VOCs. Altogether, CH_3-SiNW FET showed the strongest $\Delta\mu_h$ responses upon exposure to all tested VOCs, followed, in succession, by $COOCH_3$-SiNW FET, COOH-SiNW FET, and C_6H_5-SiNW FET.

I_{on}/I_{off} Changes of SiNW FETs upon Exposure to VOCs. The I_{on}/I_{off} changes (i.e., $\Delta(I_{on}/I_{off})$) of SiNW FETs upon exposure to VOCs were extracted and plotted (Figure 5). Excluding $COOCH_3$-SiNW FET, neither the bare (not shown) nor the molecularly modified SiNW FETs showed $\Delta(I_{on}/I_{off})$ dependence on VOC concentration (Figure 5). In most cases, it was hard to evaluate the changes because of large deviation of signals. Thus, $\Delta(I_{on}/I_{off})$ cannot be used for evaluating the molecularly modified SiNW FET sensors in the current study.

DISCUSSION

Effect of the Molecular Modification on the SiNW FETs. Assembled polar molecules on a semiconductor surface can form a dipole layer, which can create a depletion layer on semiconductor and tune the work function of semiconductors by changing electron affinity and band bending on the molecule−semiconductor interface.[36,38,42,53−55] To investigate the effect of molecular modifications on the work function of the FET's channel, bare SiNWs and molecularly modified SiNW samples were measured by Kelvin Probe. The change of work function ($\Delta\Phi$), namely, the work function of the molecularly modified SiNWs as compared to the work function of the bare SiNWs, was calculated and listed in Table 3. The

Table 3. Summary of the Work Function Changes ($\Delta\Phi$) upon Attaching a Molecular Layer (ML) to the SiNW Samples and Threshold Voltage Changes ($\Delta V_{th\text{-}ML}$) Due to the Attachment of the Molecular Layer to the SiNW FETs

molecular modification	$\Delta\Phi$ (meV)	$\Delta V_{th\text{-}ML}$ (V)
CH_3-APTES	−64.1 ± 15.0	−2.4 ± 0.2
C_5H_6-APTES	−159.5 ± 25.4	−7.6 ± 0.5
COOH-APTES	−41.1 ± 18.3	−3.1 ± 0.3
$COOCH_3$-APTES	−143.7 ± 20.4	−4.8 ± 0.2

changes of V_{th} of the examined devices, i.e., the difference between the V_{th} of the molecularly modified SiNW FET and the constituent value of the bare sample, were also listed in Table 3.

The $\Delta\Phi$ is equal to the potential drop (V_{ML}) over a surface ML-induced dipole layer (where, ML stands for molecular layer), according to:[56]

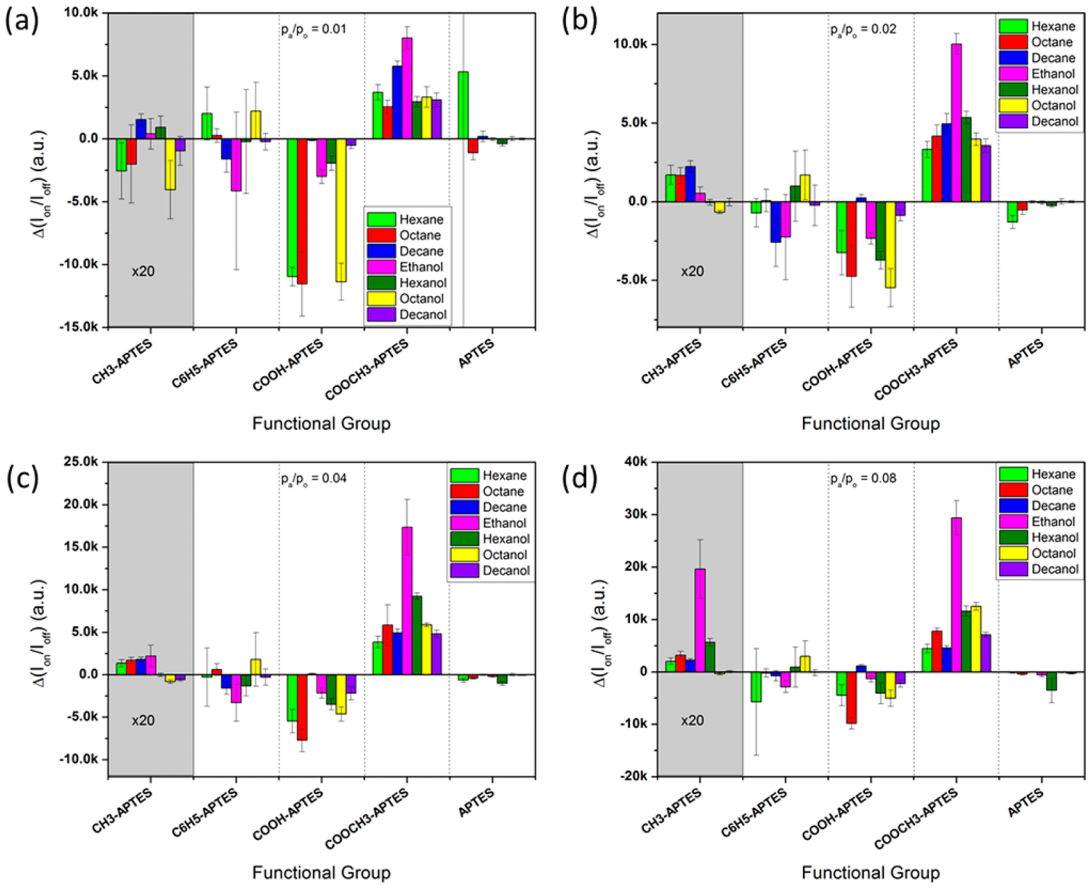

Figure 5. $\Delta(I_{on}/I_{off})$ of bare and molecularly modified SiNW FETs upon exposure to nonpolar alkyls and polar alcohols at: (a) p_a/p_o = 0.01; (b) p_a/p_o = 0.02; (c) p_a/p_o = 0.04; and (d) p_a/p_o = 0.08. For the sake of clear presentation, the data for CH_3-SiNW FET were multiplied by 20.

$$\Delta\Phi = V_{ML} = \frac{N\mu_{ML}\cos\theta}{\varepsilon_0\varepsilon_{ML}} \tag{3}$$

where N is the packing density, ε_{ML} is the relative permittivity of the ML, ε_0 is the permittivity of free space, θ is the average tilt of molecules relative to the surface normal, and μ_{ML} is the dipole moment induced by the ML. *NOTE:* the dipole moment is a vector, oriented from the (−) to the (+) charge. Here, we define negative dipole as a molecule whose negative pole is closest to the substrate than its positive one. As shown in Table 3, the work function values of all the molecularly modified SiNW samples were lower than the bare SiNW samples (i.e., $\Delta\Phi < 0$). According to eq 3, the dipole moments of all molecular layers are negative ($\mu_{ML} < 0$). Additionally, the V_{th} of all SiNW FETs were shifted to the negative side ($\Delta V_{th\text{-}ML} < 0$) after the attachment of the molecular layer (Table 3). These facts suggest that negative dipole moment of the molecular layer introduces negative V_{th} shifts to the SiNW FETs.

Dipole Sensing Model-Based Analysis. The electrostatic field of the molecular layer can induce charge carriers in the SiNW interface. The charge carrier density induced by molecular layer (Q_{ML}) is given by:

$$Q_{ML} = -C_{ML}V_{ML} = -\frac{\varepsilon_0\varepsilon_{ML}}{d}V_{ML} \tag{4}$$

where C_{ML} and d are the capacitance and thickness of the ML layer, respectively. For an accumulation conduction FET device, V_{th} is the V_g value at which the bottom SiNW surface potential is essentially zero (flat band).[57] Thus, V_{th} of molecularly modified SiNW FET exposed to dry air and exposed to analytes is given by:

$$V_{th}^{a} = \phi_{ms} - \frac{Q_{BOX}}{C_{BOX}} - \frac{Q_D}{C_{BOX}} - \frac{Q_{ML}}{C_{BOX}} \tag{5}$$

$$V_{th}^{e} = \phi_{ms} - \frac{Q_{BOX}}{C_{BOX}} - \frac{Q_D}{C_{BOX}} - \frac{Q'_{ML}}{C_{BOX}} \tag{6}$$

where ϕ_{ms} is the difference between the work function of the gate material and of the SiNW, Q_{BOX} is the sum of all (fixed and trapped) charges in the back oxide of the substrate, Q_D is the absolute charge at the SiNW depletion layer that is induced by back gate bias voltage, Q_{ML} is the charge carrier induced by the SiNW FET's molecular layer upon exposure to dry air, and Q'_{ML} is the charge carrier induced by the SiNW FET's molecular layer upon exposure to analyte. Hence, the V_{th} change induced by analyte exposure can be expressed:

$$\Delta V_{th} = V_{th}^{e} - V_{th}^{a} = -\frac{Q'_{ML} - Q_{ML}}{C_{BOX}} \tag{7}$$

Using eqs 3 and 4, eq 7 can be rewritten as

$$\Delta V_{th} = \frac{N}{dC_{BOX}}(\mu'_{ML}\cos\theta' - \mu_{ML}\cos\theta) \tag{8}$$

where μ'_{ML} and θ' are the dipole moment and the average tilt angle of the molecular layer upon exposure of the device to analyte, respectively.

dx.doi.org/10.1021/am4004649 | ACS Appl. Mater. Interfaces 2013, 5, 2289−2299

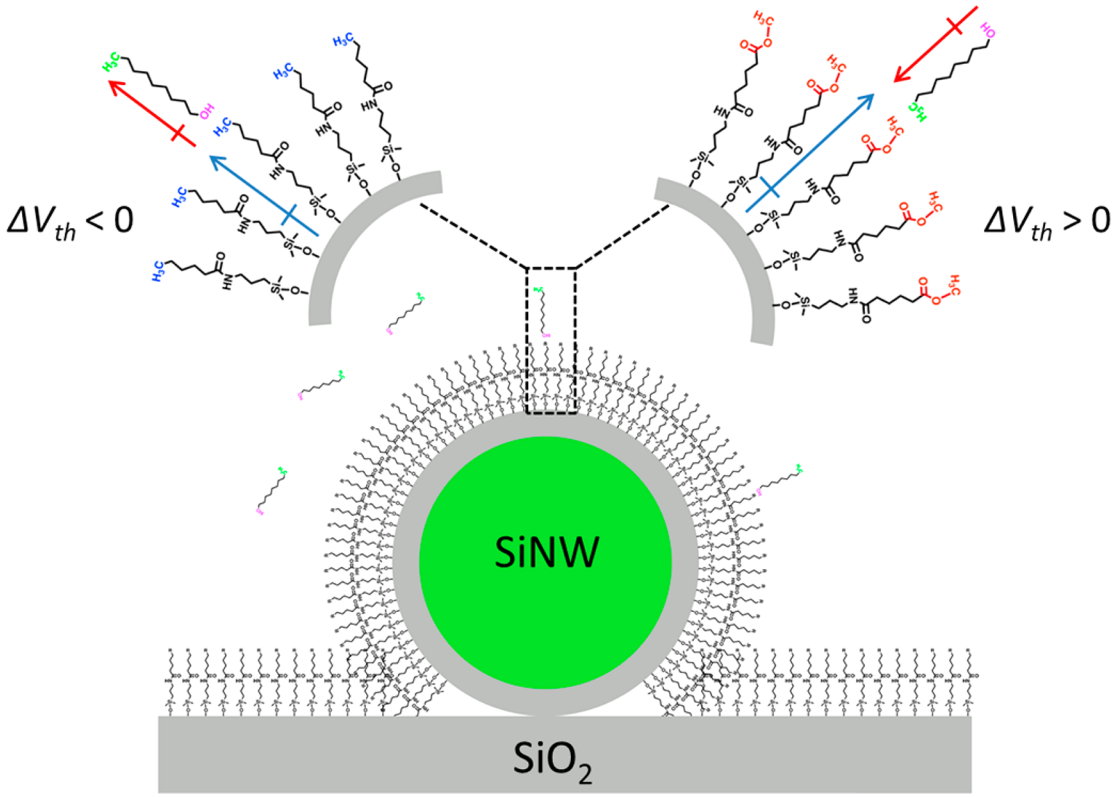

Figure 6. Schematics demonstration of (a) CH_3-SiNW FET and (b) $COOCH_3$-SiNW FET upon exposure to polar VOCs.

Adsorption of VOC on molecular layer can be classified into two types: (a) adsorption on the molecular layer's surface and (b) diffusion between the chains of the molecular layer. For case (a), if the VOC is nonpolar, the adsorption is primarily driven by induced dipole (nonpolar VOC)−dipole (polar ML) interaction; if the VOC is polar, the adsorption is primarily driven by dipole−dipole interaction between the polar ML surface and polar VOC. When VOC adsorbs on the molecular layer's surface, the VOC is attached to the exposed functional groups. Thus, the alignment of VOC on the molecular layer's surface is controlled by the properties of molecular functional groups. For instance, CH_3 and C_6H_5 are electron donating groups. In these cases, the VOC's negative pole is attached on the molecular layer's surface (Figure 6a). Under these circumstances, the dipole moment orientation of the adsorbed VOCs is similar to the molecular layer. As a result, adsorption of VOCs increase the absolute value of the molecular layer's dipole moment ($|\mu'_{ML}| > |\mu_{ML}|$). Let us suppose that the molecular layer has no tilt after VOC adsorption. This dipole moment decrease shall make a V_{th} shift according to eq 8. Since the dipole moments of various molecular layers are negative, V_{th} will shift to negative side ($\Delta V_{th} < 0$).

In contrast to the CH_3 and C_6H_5 functional groups, COOH and $COOCH_3$ end groups are electron withdrawing. In this case, the positive pole of the VOC is attached to the molecular layer's surface (Figure 6b) and the dipole moment orientation of adsorbed VOC is opposite to that of molecular layers, generating a decrease of the absolute value of molecular layer's dipole moment ($|\mu'_{ML}| < |\mu_{ML}|$). According to eq 8, V_{th} will shift to the positive side, fitting with our experiment data.

Polar (alcohol) VOCs might selectively attach to the functional group of the molecular layer, either through the methyl (positive pole) part or through the hydroxyl (negative pole) part. For molecular layers with electron-donating functional groups (CH_3 and C_5H_6), it is likely that the adsorption process occurs through interaction between the hydroxyl part of the VOC and the functional group of the molecular layer. For molecular layers with electron-withdrawing functional groups (COOH and $COOCH_3$), it is likely that the adsorption process occurs through interaction between the methyl part of the VOC and the functional group of the molecular layer. An exceptional case is the COOH-SiNW FET upon exposure to polar alcohols. In this case, the hydroxyl part of the alcohol VOC is likely attached to the COOH-SiNW surface via a strong hydrogen bond with the COOH functional group of the molecular layer because the hydrogen bond interaction is stronger than dipole−dipole interaction between the methyl part of VOC and COOH-SiNW surface. The strong hydrogen bond interaction between the alcohol VOCs and COOH-SiNW surface could be evidenced (though, indirectly) from the slow desorption process of alcohol VOCs during the dry airflow step applied in our study (Figure S4, Supporting Information). Finally, since the dipole−dipole interaction is always stronger than induced dipole−dipole interaction, adsorption of polar VOCs can lead to a larger change of dipole moment than nonpolar VOCs, thus explaining the higher ΔV_{th} changes achieved for polar VOCs, compared to nonpolar VOCs with similar chain length.

For case (b), when the VOC is diffused between the chains of molecular layer, repulsive forces induced by the VOCs shall tilt the molecules of the molecular layer. If $\theta' > \theta$, then $\cos\theta' < \cos\theta$ ($0° \leq \theta < \theta' \leq 90°$). Let us suppose that the dipole moment of the molecular layer remains constant during the diffusion process of the VOC. According to eq 8, if $\theta' > \theta$, the dipole moment of the molecular layer leads to $\Delta V_{th} > 0$. In contrast, if $\theta' < \theta$, the dipole moment of the molecular layer

dx.doi.org/10.1021/am4004649 | ACS Appl. Mater. Interfaces 2013, 5, 2289−2299

leads to $\Delta V_{th} < 0$. However, practically, VOCs that are diffused into the chains of the molecular layers can simultaneously decrease the titling angle of part of the molecules within the molecular layer while increasing the titling angle of the other part. Ultimately, these two simultaneous (opposite) effects can be compensated with each other, thus weakening the ΔV_{th} response generated by VOC diffusion. According to our experimental results, we infer that adsorption of VOC on top of the molecular layer has more significant effect on the ΔV_{th}, as compared with the effect resulting from the VOC diffusion within the molecular layer.

According to the above-mentioned dipole-induced sensing model, the end groups of molecular layers act as "antennas" for VOCs. Therefore, it can be inferred that the higher the density of end groups, the stronger is the ΔV_{th} response. This argument might explain why SiNW FETs with CH_3-APTES and $COOCH_3$-APTES (which have higher density of functional groups than that of C_6H_5-APTES and COOH-APTES) exhibit stronger ΔV_{th} responses (see Figure 3).

Carrier Mobility. The increase of $\Delta\mu_h$ upon exposure to VOCs were reported for silane-terminated SiNW FET and InAs NW FET-based gas sensors.[21,58] The increase in $\Delta\mu_h$ was attributed to a decrease in the density of the negatively charged surface states upon the adsorption of the VOCs.[21] Our results showed that $\Delta\mu_h$ was independent from ΔV_{th}. For instance, COOH-SiNW FET showed no ΔV_{th} response to polar VOCs at high VOC concentrations, but it showed positive $\Delta\mu_h$ response under the same condition. Similar to the discussion in the previous section, the functional groups of the COOH-APTES molecular layer were saturated by adsorbed alcohol VOCs after the first exposure cycle. Therefore, we ascribe the $\Delta\mu_h$ response mainly to the VOC diffusion between the chains of molecular layer that is attached to the SiNW FET (case b).

The dependence of the $\Delta\mu_h$ response on the functional groups (CH_3-SiNW FET > $COOCH_3$-SiNW FET > COOH-SiNW FET > C_6H_5-SiNW FET) can be explained by differences in the VOC wettability of the molecular layers.[59,60] For example, CH_3-APTES has similar structure to the tested VOCs, and therefore, it facilitates the adsorption and diffusion of the VOCs between the chains of molecular layer.[59,60] This would explain why CH_3-SiNW FET exhibited the strongest $\Delta\mu_h$ response, among all tested devices. C_6H_5-APTES has low wettability for both alcohols and alkyls, making the diffusion of the VOCs into the interspace of the molecular layer rather difficult. This would explain why C_6H_5-SiNW FET exhibited the weakest $\Delta\mu_h$ response among all tested devices.

SUMMARY AND CONCLUSIONS

We have provided experimental results showing that SiNW FETs that are modified with polar molecular layers could detect both polar and nonpolar VOCs. The results show that V_{th} and μ_h are two efficient parameters to evaluate the sensitivity of molecularly modified SiNW FETs toward VOCs. The ΔV_{th} and $\Delta\mu_h$ responses show strong dependence with the VOC concentration and, also, reversible sensing characteristics. Model-based analysis indicates that the interaction between the molecular layers and the VOCs can be classified to three main cases: (a) dipole−dipole interaction between the molecular layer and the polar VOCs; (b) induced dipole−dipole interaction between the molecular layers and the nonpolar VOCs; and (c) molecule tilt as a result of VOCs diffusion between the chains of molecular layer. These three scenarios were shown to contribute to changes in the dipole moment of the molecular layer and, as a result, to ΔV_{th}. The electron-donating or electron-withdrawing properties of the functional groups were shown to control the dipole moment orientation of the adsorbed VOCs and, as a result, was the main reason determining the direction (or sign) of the ΔV_{th}. The potential diffusion of the VOCs between the chains of molecular layer, determined by the type and density of the functional groups, was shown to be the main reason for the $\Delta\mu_h$ responses. The reported findings and sensing model are expected to provide an efficient way to design chemical sensors that are based on SiNW FETs. Of special interest, the reported findings would be very helpful for designing molecular layers serving as chemical antennas for nonpolar VOCs, which do not exchange direct charge transfer with the SiNW FET. Complementary understanding of the mutual effects between the molecular layers and VOCs could be achieved by systematic variation of the molecular backbone length and systematic variation of the binding groups to the SiNW surface. Utilizing beveled SiO_2 sheath around the SiNWs would provide further valuable understanding on the sensing-related electrostatics.

ASSOCIATED CONTENT

Supporting Information

Method for synthesizing 5-phenylvaleric chloride, dark field optical microscope image of SiNW mat, XPS spectra of molecularly modified SiNWs, V_{th} response of sensor COOH-SiNW FET to hexanol, and ΔV_{th} and $\Delta\mu_h$ of bare-SiNW FET sensor upon exposure to VOCs. This material is available free of charge via the Internet at http://pubs.acs.org.

AUTHOR INFORMATION

Corresponding Author

*E-mail: hhossam@tx.technion.ac.il.

Notes

The authors declare no competing financial interest.

ACKNOWLEDGMENTS

The research leading to these results has received funding from the FP7-Health Program under the LCAOS (grant agreement 258868). The authors acknowledge the "Israel Council for Higher Education" for a partial support of Bin Wang's postdoctoral fellowship and Dr. Silke Christiansen (Max-Planck-Institute for the Science of Light, Germany) for providing part of the SiNWs reported in the current study.

REFERENCES

(1) Li, D.; Song, S.; Fan, C. *Acc. Chem. Res.* **2010**, *43*, 631.
(2) Liu, L.; Shao, M.; Lee, S.-T. *J. Nanoeng. Nanomanuf.* **2012**, *2*, 102.
(3) Stern, E.; Vacic, A.; Reed, M. A. *IEEE Trans. Electron Devices* **2008**, *55*, 3119.
(4) Wanekaya, A. K.; Chen, W.; Myung, N. V.; Mulchandani, A. *Electroanalysis* **2006**, *18*, 533.
(5) Penner, R. M. *Ann. Rev. Anal. Chem.* **2012**, *5*, 461.
(6) Schmidt, V.; Wittemann, J. V.; Gosele, U. *Chem. Rev.* **2010**, *10*, 361.
(7) Wang, D.; Sheriff, B. A.; MacAlpine, M.; Health, J. R. *Nano Res.* **2008**, *1*, 9.
(8) He, X. D.; Guo, C. S.; Liu, Y.; Tsang, C. H. A.; Ma, D. D. D.; Zhang, R. Q.; Wong, N. B.; Kang, Z. H.; Lee, S. T. *Appl. Phys. Lett.* **2011**, *98*, 043108.
(9) Collins, G.; Holmes, J. D. *J. Mater. Chem.* **2011**, *21*, 11052.
(10) Puniredd, S. R.; Assad, O.; Stelzner, T.; Christiansen, S.; Haick, H. *Langmuir* **2011**, *27*, 4764.

(11) Assad, O.; Puniredd, S. R.; Stelzner, T.; Christiansen, S.; Haick, H. *J. Am. Chem. Soc.* **2008**, *130*, 17670.
(12) Bashouti, M. Y.; Paska, Y.; Puniredd, S. R.; Stelzner, T.; Christiansen, S.; Haick, H. *Phys. Chem. Chem. Phys.* **2009**, *11*, 3845.
(13) Bashouti, M. Y.; Stelzner, T.; Berger, A.; Christiansen, S.; Haick, H. *J. Phys. Chem. C* **2008**, *112*, 19168.
(14) Bashouti, M. Y.; Stelzner, T.; Berger, A.; Christiansen, S.; Haick, H. *J. Phys. Chem. C* **2009**, *113*, 14823.
(15) Bashouti, M. Y.; Tung, R. T.; Haick, H. *Small* **2009**, *5*, 2761.
(16) Zhou, X. T.; Hu, J. Q.; Li, C. P.; Ma, D. D. D.; Lee, C. S.; Lee, S. T. *Chem. Phys. Lett.* **2003**, *369*, 220.
(17) McAlpine, M. C.; Ahmad, H.; Wang, D. W.; Heath, J. R. *Nat. Mater.* **2007**, *6*, 379.
(18) Engel, Y.; Elnathan, R.; Pevzner, A.; Davidi, G.; Flaxer, E.; Patolsky, F. *Angew. Chem., Int. Ed.* **2010**, *49*, 6830.
(19) Jonas, F.; Frank, K. K.; Karen, C. C. *Sensors (Basel, Switzerland)* **2009**, *9*, 9196.
(20) Paska, Y.; Haick, H. *ACS Appl. Mater. Interfaces* **2012**, *4*, 2604.
(21) Paska, Y.; Stelzner, T.; Assad, O.; Tisch, U.; Christiansen, S.; Haick, H. *ACS Nano* **2012**, *6*, 335.
(22) Paska, Y.; Stelzner, T.; Christiansen, S.; Haick, H. *ACS Nano* **2011**, *5*, 5620.
(23) He, B.; Morrow, T. J.; Keating, C. D. *Curr. Opin. Chem. Biol.* **2008**, *12*, 522.
(24) Ramgir, N. S.; Yang, Y.; Zacharias, M. N. *Small* **2010**, *6*, 1705.
(25) He, T.; Corley, D. A.; Lu, M.; Di Spigna, N. H.; He, J. L.; Nackashi, D. P.; Franzon, P. D.; Tour, J. M. *J. Am. Chem. Soc.* **2009**, *131*, 10023.
(26) Takulapalli, B. R. *ACS Nano* **2010**, *4*, 999.
(27) Hakim, M.; Broza, Y. Y.; Barash, O.; Peled, N.; Phillips, M.; Amann, A.; Haick, H. *Chem. Rev.* **2012**, *112*, 5949.
(28) Tisch, U.; Billan, S.; Ilouze, M.; Phillips, M.; Peled, N.; Haick, H. *CML-Lung Cancer* **2012**, *5*, 107.
(29) Tisch, U.; Haick, H. *Rev. Chem. Eng.* **2010**, *26*, 171.
(30) Tisch, U.; Haick, H. *MRS Bull.* **2010**, *35*, 797.
(31) Kneepkens, C. M. F.; Lepage, G.; Roy, C. C. *Free Radical Biol. Med.* **1994**, *17*, 127.
(32) Barash, O.; Peled, N.; Hirsch, F. R.; Haick, H. *Small* **2009**, *5*, 2618.
(33) Barash, O.; Peled, N.; Tisch, U.; Bunn, P. A.; Hirsch, F. R.; Haick, H. *Nanomedicine (New York, NY, US)* **2012**, *8*, 580.
(34) Amal, H.; Ding, L.; Liu, B. B.; Tisch, U.; Xu, Z. Q.; Shi, D. Y.; Zhao, Y.; Chen, J.; Sun, R. X.; Liu, H.; Ye, S. L.; Tang, Z. Y.; Haick, H. *Int. J. Nanomed.* **2012**, *7*, 4135.
(35) Boudinet, D.; Benwadih, M.; Altazin, S.; Verilhac, J.-M.; De Vito, E.; Serbutoviez, C.; Horowitz, G.; Facchetti, A. *J. Am. Chem. Soc.* **2011**, *133*, 9968.
(36) He, T.; He, J. L.; Lu, M.; Chen, B.; Pang, H.; Reus, W. F.; Nolte, W. M.; Nackashi, D. P.; Franzon, P. D.; Tour, J. M. *J. Am. Chem. Soc.* **2006**, *128*, 14537.
(37) Huang, C.; Katz, H. E.; West, J. E. *Langmuir* **2007**, *23*, 13223.
(38) Kobayashi, S.; Nishikawa, T.; Takenobu, T.; Mori, S.; Shimoda, T.; Mitani, T.; Shimotani, H.; Yoshimoto, N.; Ogawa, S.; Iwasa, Y. *Nat. Mater.* **2004**, *3*, 317.
(39) Shaya, O.; Shaked, M.; Usherenko, Y.; Halpern, E.; Shalev, G.; Doron, A.; Levy, I.; Rosenwaks, Y. *J. Phys. Chem. C* **2009**, *113*, 6163.
(40) Wang, A.; Kymissis, I.; Bulović, V.; Akinwande, A. I. *Appl. Phys. Lett.* **2006**, *89*, 112109.
(41) Salinas, M.; Jäger, C. M.; Amin, A. Y.; Dral, P. O.; Meyer-Friedrichsen, T.; Hirsch, A.; Clark, T.; Halik, M. *J. Am. Chem. Soc.* **2012**, *134*, 12648.
(42) Ashkenasy, G.; Cahen, D.; Cohen, R.; Shanzer, A.; Vilan, A. *Acc. Chem. Res.* **2002**, *35*, 121.
(43) Li, Y.; Calder, S.; Yaffe, O.; Cahen, D.; Haick, H.; Kronik, L.; Zuilhof, H. *Langmuir* **2012**, *28*, 9920.
(44) Patolsky, F.; Zheng, G. F.; Lieber, C. M. *Nat. Protoc.* **2006**, *1*, 1711.
(45) Stelzner, T.; Andra, G.; Wendler, E.; Wesch, W.; Scholz, R.; Gosele, U.; Christiansen, S. *Nanotechnology* **2006**, *17*, 2895.
(46) Assad, O.; Leshansky, A. M.; Wang, B.; Stelzner, T.; Christiansen, S.; Haick, H. *ACS Nano* **2012**, *6*, 4702.
(47) Wang, B.; Stelzner, T.; Dirawi, R.; Assad, O.; Shehada, N.; Christiansen, S.; Haick, H. *ACS Appl. Mater. Interfaces* **2012**, *4*, 4251.
(48) Konvalina, G.; Haick, H. *ACS Appl. Mater. Interfaces* **2012**, *4*, 317.
(49) Zilberman, Y.; Ionescu, R.; Feng, X.; Mullen, K.; Haick, H. *ACS Nano* **2011**, *5*, 6743.
(50) Zilberman, Y.; Tisch, U.; Shuster, G.; Pisula, W.; Feng, X.; Mullen, K.; Haick, H. *Adv. Mater.* **2010**, *22*, 4317.
(51) Haynes, W. M. *CRC Handbook of Chemistry and Physics*, 91st ed.; CRC Press: Boulder, CO, 2010−2011.
(52) Wanger, C. D.; Riggs, W. M.; Davis, L. E.; Moulder, J. F.; Muilenberg, G. E. *Handbook of X-Ray Photoelectron Spectroscopy*; Perkin-Elmer Corp.: Eden Prairie, Minnesota, USA, 1979.
(53) Cahen, D.; Naaman, R.; Vager, Z. *Adv. Funct. Mater.* **2005**, *15*, 1571.
(54) Peor, N.; Sfez, R.; Yitzchaik, S. *J. Am. Chem. Soc.* **2008**, *130*, 4158.
(55) Salinas, M.; Jager, C. M.; Amin, A. Y.; Dral, P. O.; Meyer-Friedrichsen, T.; Hirsch, A.; Clark, T.; Halik, M. *J. Am. Chem. Soc.* **2012**, *134*, 12648.
(56) Moench, W. *Semiconductor Surfaces and Interfaces*, 3rd ed.; Springer-Verlag: Berlin, Germany, 2001.
(57) Sze, S. M. *Semiconductor Devices: Physics and Technology*, 2nd ed.; John Wily & Sons, Inc.: Chichester, UK, 2001.
(58) Du, J.; Liang, D.; Tang, H.; Gao, X. P. A. *Nano Lett.* **2009**, *9*, 4348.
(59) Ulman, A. *Chem. Rev.* **1996**, *96*, 1533.
(60) Tsukruk, V. V. *Adv. Mater.* **2001**, *13*, 95.